

EPJ manuscript No.  
(will be inserted by the editor)

# Updated dispersion-theoretical analysis of the nucleon electromagnetic form factors<sup>\*</sup>

H.-W. Hammer<sup>1,a,b</sup> and Ulf-G. Meißner<sup>1,2,c</sup>

<sup>1</sup> Universität Bonn, Helmholtz-Institut für Strahlen- und Kernphysik (Theorie), D-53115 Bonn, Germany

<sup>2</sup> Forschungszentrum Jülich, Institut für Kernphysik (Theorie), D-52425 Jülich, Germany

Received: date / Revised version: date

**Abstract.** In the light of the new data on the various neutron and proton electromagnetic form factors taken in recent years, we update the dispersion-theoretical analysis of the nucleon electromagnetic form factors from the mid-nineties. The parametrization of the spectral functions includes constraints from unitarity, perturbative QCD, and recent measurements of the neutron charge radius. We obtain a good description of most modern form factor data, with the exception of the Jefferson Lab data on  $G_E^p/G_M^p$  in the four-momentum transfer range  $Q^2 = 3...6$  GeV<sup>2</sup>. For the magnetic radii of the proton and the neutron we find  $r_M^p = 0.857$  fm and  $r_M^n = 0.879$  fm, which is consistent with the recent determinations using continued fraction expansions.

**PACS.** 13.40.Gp, 11.55.Fv, 13.60.Fz

## 1 Introduction

The electromagnetic form factors of the nucleon encode information about the structure of the nucleon over a wide range of scales. Depending on the kinematical conditions, they can be determined most precisely from elastic electron scattering using Rosenbluth-separation or in double polarization experiments. Only in the last decade has it become technically feasible to perform the double polarization experiments. Thus the data base has been considerably enlarged since our last dispersion analysis was performed in 1996 [1,2]. This holds in particular for the neutron form factors, which can only be measured indirectly using deuterium or <sup>3</sup>He targets. For recent reviews, see e.g. Refs. [3,4]. At low momentum transfer, one obtains information about the various nucleon rms-radii, which are not only of interest by themselves but e.g. the proton charge radius  $r_E^p$  has also to be known to a good accuracy to perform precision tests of QED in Lamb-shift measurements, or conversely, one can use such experiments to pin down  $r_E^p$ . For some time, low-energy electron scattering and Lamb shift determinations led to different values for  $r_E^p$ , but this discrepancy has been resolved, see Refs. [5,6] and references therein. One can also extract vector meson–nucleon coupling constants and eventually study the tran-

sition from the non-perturbative regime of QCD to the perturbative one. Since the data span the range of four-momentum transfers from  $Q^2 \simeq 0$  to  $Q^2 \simeq 31$  GeV<sup>2</sup>, the only model-independent method to analyze these data is dispersion theory. The most recent dispersion-theoretical analysis of the nucleon electromagnetic form factors dates back to almost a decade ago, including fits to space-like [1] as well as time-like data [2]. For some recent vector-meson pole-model approaches to the nucleon electromagnetic form factors, see Refs. [7,8]. In view of the new data and a new data base collected and discussed in Ref. [9], it seems timely to update the work of Refs. [1,2] using the data basis of [9]. It is also interesting to investigate whether such a general scheme can lead to the pronounced structure around  $Q^2 = 0.2$  GeV<sup>2</sup> found for all four form factors in the phenomenological analysis of Ref. [9].

## 2 Formalism

The electromagnetic structure of the nucleon is parameterized by the Dirac ( $F_1$ ) and Pauli ( $F_2$ ) form factors for the proton and the neutron

$$F_i^{p/n}(Q^2) = F_i^S(Q^2) \pm F_i^V(Q^2), \quad i = 1, 2, \quad (1)$$

with  $Q^2$  the four-momentum transfer of the virtual photon (the photon virtuality). Our conventions are such that  $Q^2 > 0$  for space-like momentum transfer. We have expressed the nucleon form factors in the isospin basis ( $S =$  isoscalar,  $V =$  isovector) which is most appropriate for the dispersive analysis. The experimental data are usually

<sup>\*</sup> Work supported in part by the DFG under contract HA 3203/2-1.

<sup>a</sup> *Present address:* Institute for Nuclear Theory, University of Washington, Seattle, WA 98195, USA

<sup>b</sup> Email: hammer@phys.washington.edu

<sup>c</sup> Email: meissner@itkp.uni-bonn.de

given for the Sachs form factors, which are linear combinations of  $F_1$  and  $F_2$ :

$$G_E^I(Q^2) = F_1^I(Q^2) - \frac{Q^2}{4m^2} F_2^I(Q^2), \quad (2)$$

$$G_M^I(Q^2) = F_1^I(Q^2) + F_2^I(Q^2), \quad I = S, V. \quad (3)$$

The analysis of the nucleon electromagnetic form factors proceeds most directly through the spectral representation given by<sup>1</sup>

$$F_i^I(Q^2) = \frac{1}{\pi} \int_{(\mu_0^I)^2}^{\infty} \frac{\sigma_i^I(\mu^2) d\mu^2}{\mu^2 + Q^2}, \quad i = 1, 2, \quad I = S, V, \quad (4)$$

in terms of the real spectral functions  $\sigma_i^I(\mu^2) = \text{Im} F_i^I(\mu^2)$ , and the corresponding thresholds are given by  $\mu_0^S = 3M_\pi$ ,  $\mu_0^V = 2M_\pi$ . The spectral functions encode the pertinent physics of the nucleon form factors. In the isovector channel, the spectral function is build up by the two-pion continuum (including the  $\rho$ -resonance) as given by unitarity [10] plus a series of poles, whose masses and residues are fit parameters. In the isoscalar channel, we only have poles, where the lowest two are given by the  $\omega$  and the  $\phi$  mesons, respectively. We restrict the number of poles in both channels by the stability condition of Ref. [11] which requires to use the minimum number of vector meson poles necessary to fit the data. Note that this condition was also used in the earlier fits [10, 1, 2]. Enforcing the correct normalization conditions for all form factors, the experimental value of the neutron charge radius and the superconvergence relations from the perturbative QCD behaviour of the form factors, e.g.  $F_i(Q^2) \sim 1/(Q^2)^{i+1}$  as  $Q^2$  tends to infinity, reduces the number of free fit parameters considerably. For more details on the form of the spectral functions, the stability condition, and the way the various constraints are included, see Ref. [1].

It is possible to take all pole masses from physical particles (except for one which is determined by the constraints discussed above). As a consequence, we have 2 (3) free parameters in the isovector (isoscalar) channel if we restrict the number of poles to 3 (4). Furthermore, we have one more free parameter that characterizes the onset of the leading logarithms from perturbative QCD. A difference to the earlier fits [1, 2] is that the constraint from the neutron charge radius has somewhat changed. While in [1, 2] an electron-neutron scattering length of  $b_{ne} = (-1.308 \pm 0.05) \cdot 10^{-3}$  fm was used, the reevaluation of the data lead to  $b_{ne} = (-1.33 \pm 0.027 \pm 0.03) \cdot 10^{-3}$  fm for scattering off  $^{208}\text{Pb}$  and  $b_{ne} = (-1.44 \pm 0.033 \pm 0.06) \cdot 10^{-3}$  fm for  $^{209}\text{Bi}$  [12]. We have performed fits with both values but only show results for the Pb value which seems to be favored by the  $G_E^n$  data.

### 3 Results

Before discussing the results, we must specify the data to which we fit. We use the data basis collected and specified by Friedrich and Walcher in Ref. [9]. It consists of a total of 190 data points, about a quarter of which were not available in 1996 (mainly for the neutron). Furthermore, the data basis has also been pruned for inconsistent data and therefore does not make use of some of the data that were included in the fits of [1, 2]. For a detailed list of the data taken into consideration, we refer the reader to Ref. [9]. In particular, the Jefferson Lab data for  $G_E^p/G_M^p$  [13, 14] are treated as data for  $G_E^p$  in [9] since  $G_M^p$  is supposed to be known better for these virtualities.

Fitting these data with the readjusted constraints leads to the following parameters. The isoscalar masses are  $M_\omega = 0.782$  GeV,  $M_\phi = 1.019$  GeV,  $M_{S'} = 1.65$  GeV, and  $M_{S''} = 1.68$  GeV. Note that in contrast to the earlier fits, we can not work with 3 isoscalar poles only. The isovector masses are  $M_{\rho'} = 1.05$  GeV,  $M_{\rho''} = 1.465$  GeV, and  $M_{\rho'''} = 1.70$  GeV. Note that except from  $M_{\rho'}$ , whose value is fixed from the various constraints, all these masses correspond to physical particles listed in the PDG tables. The corresponding residua for the isoscalar poles are:  $a_1^\omega = 0.767$ ,  $a_2^\omega = 0.318$ ,  $a_1^\phi = -0.832$ ,  $a_2^\phi = -0.250$ ,  $a_1^{S'} = 2.09$ ,  $a_2^{S'} = 3.97$ ,  $a_1^{S''} = -2.04$ , and  $a_2^{S''} = -3.76$ , where the subscript 1 (2) refers to the vector (tensor) coupling of the corresponding vector meson to the nucleon. Similarly, we have for the three isovector poles:  $a_1^{\rho'} = -0.154$ ,  $a_2^{\rho'} = -0.306$ ,  $a_1^{\rho''} = 1.15$ ,  $a_2^{\rho''} = -4.42$ ,  $a_1^{\rho'''} = -1.32$ , and  $a_2^{\rho'''} = 3.18$ . The QCD parameters (for definitions, see [1]) are  $\gamma = 2.148$ ,  $\Lambda^2 = 18.28$  GeV<sup>2</sup> and  $Q_0^2 = 0.35$  GeV<sup>2</sup>. The value of  $\Lambda^2$  characterizes the onset of the leading logarithmic behavior from perturbative QCD. We note that the value for  $\Lambda^2$  chosen here is about a factor of two larger than in the earlier fits [1, 2]. This change is due to the strong deviation of the new Jefferson Lab data for  $G_E^p/G_M^p$  [13, 14] from the asymptotic prediction of perturbative QCD.

The errors in the fit parameters quoted above are unknown. Due to the highly nonlinear nature of the problem (remember that we fit all 4 form factors simultaneously) a trustworthy error analysis is a very non-trivial problem. This is complicated by the fact that the errors of some inputs (e.g. the two-pion continuum [10]) are not known. For this reason, no errors were given in the previous dispersion analyses by Höhler et al. [15] and Mergell et al. [1] (and also not in the widely used dispersion theoretical analysis of pion-nucleon scattering by Höhler and coworkers [16]). At present, it is an open problem how to assign a serious theoretical error to such type of analysis.

In the previous dispersion analyses [1, 2], a strong fine tuning of the residues of the excited  $\rho$  mesons in the isovector channel could be observed. It is well known that the experimental dipole behavior of the form factors requires two narrow structures with opposite signs close to each other. The fits in the previous analyses, however, tended to favor very large residues ( $\sim 40$ ) for a small overall gain in  $\chi^2$ . Taken at face value, these residues implied unphys-

<sup>1</sup> Note that we work with unsubtracted dispersion relations. Since the normalizations of the various form factors are known, one could also work with once-subtracted dispersion relations.

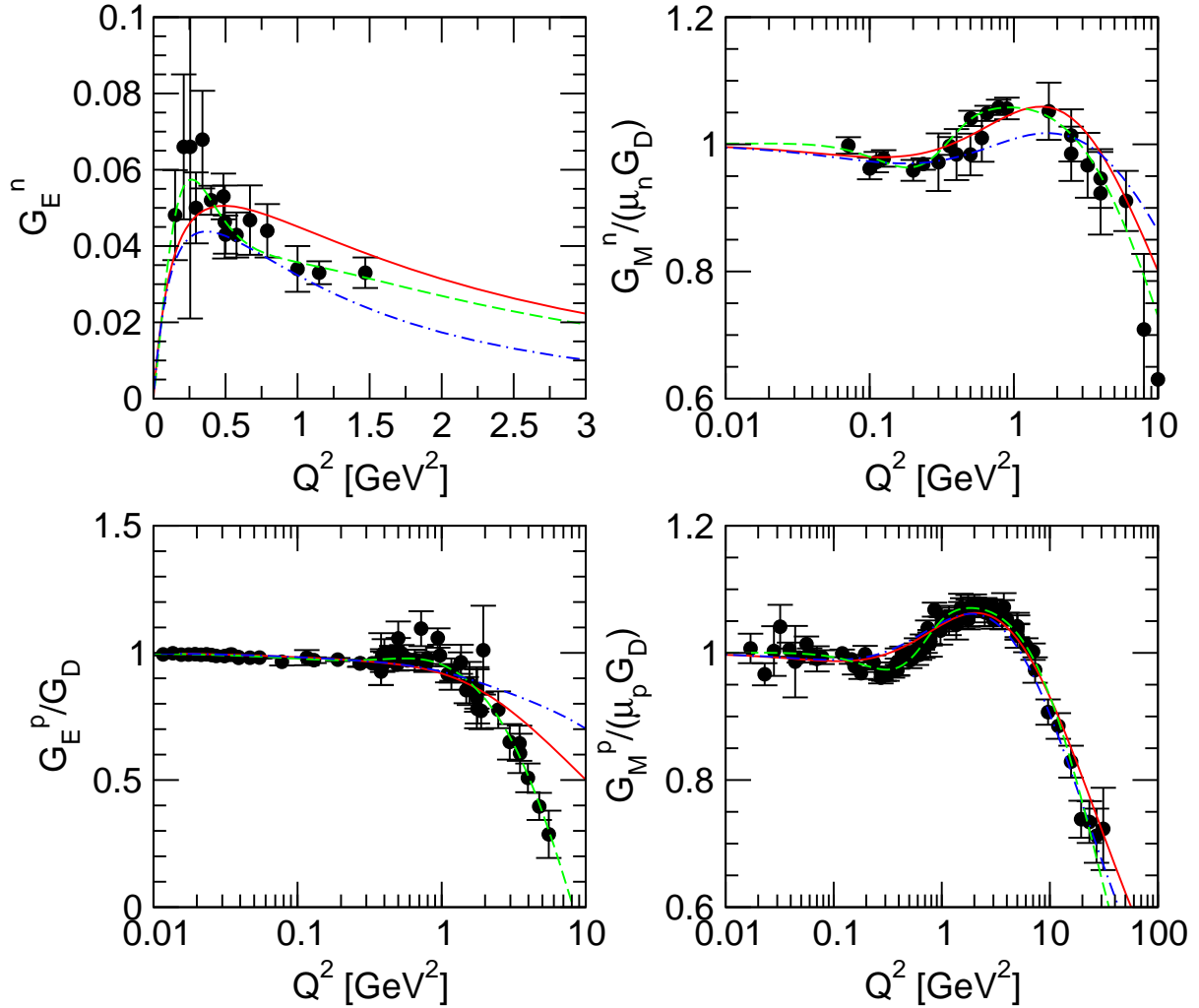


**Fig. 1.** The nucleon form factors for space-like momentum transfer. The solid line gives our best fit for  $b_{ne} = (-1.33 \pm 0.027 \pm 0.03) \cdot 10^{-3}$  fm [12] while the dash-dotted line gives fit 1 from Ref. [2]. The dashed lines give the result of the phenomenological fit of Ref. [9].

ically large couplings for the isovector poles to the nucleon. In order to avoid this problem, we have restricted the magnitude of the vector meson coupling constants in the present analysis. As a consequence, the residues of all poles in the isoscalar and isovector channels are of order one.

In Fig. 1, we show the resulting Sachs form factors by the solid line. The form factors are normalized to the canonical dipole fit, with the exception of the neutron electric form factor, which is not scaled. We can describe most of the data fairly well, with the exception of the Jefferson Lab data on  $G_E^p$  in the  $Q^2$  range from 3 to 6  $\text{GeV}^2$  (see also the discussion in Refs. [17,18]). The  $\chi^2/\text{datum}$  of this fit is 2.07. For comparison, we exhibit fit 1 of Ref. [2] by the dash-dotted line. This fit is based on the 1996 data basis and describes the data clearly worse than our new fit. Also shown by the dashed line is the fit with the “phenomenological ansatz” of [9], which has 6 free parameters

for each of the 4 form factors.<sup>2</sup> It does significantly better for  $G_E^p$ . In Ref. [9], a number of other fits with a “physically motivated ansatz” were also performed. These fits are generally comparable in quality to the one shown in Fig. 1 but give a better description of  $G_M^p$ .

In the fits of Ref. [9], a pronounced structure around  $Q^2 \simeq 0.2 \text{ GeV}^2$  was found for  $G_E^n$  (and could also be isolated in the other form factors as a small effect). This region of momentum transfers is shown in Fig. 2 in greater detail. The structure was attributed to a contribution from a very long range pion cloud (for a discussion of this point,

<sup>2</sup> We have reproduced this fit from Eqs. (4-6) and the numbers given in Table 2 of the published version of Ref. [9]. For  $G_M^p$ , we have used the following values for the parameters:  $a_{10} = 1.0024$ ,  $a_{11} = 0.7554$ ,  $a_{20} = 1.0000 - a_{10} = -0.0024$ ,  $a_{21} = 14.68$ ,  $a_b = -0.159$ ,  $Q_b = 0.325$ ,  $\sigma_b = 0.231$  which differ slightly from what is given in Table 2 of the published version of Ref. [9]. With the numbers in that table, one can not reproduce the curve shown in Fig. 4 of [9].

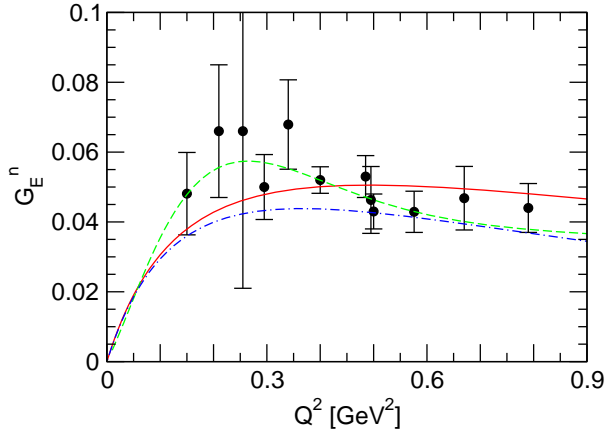


**Fig. 2.** The neutron charge form factor  $G_E^n$  for momentum transfers  $Q^2 = 0 \dots 0.9 \text{ GeV}^2$ . The curves are as in Fig. 1.

see also Ref. [19]). Our analysis does not show the pronounced structure around  $Q^2 \simeq 0.2 \text{ GeV}^2$ . What this result means remains to be seen. Taking the errors of the experimental data into account, the structure is not an unambiguous feature of the data (cf. Fig. 2). Ultimately, the question of whether the structure found in Ref. [9] is real physics or not should be decided by more accurate data in the region  $Q^2 \simeq 0.2 \text{ GeV}^2$ . A similar plot for the proton charge form factor in the low momentum transfer region is shown in Fig. 3. The data in this range are sufficiently spread to leave room for various interpretations.

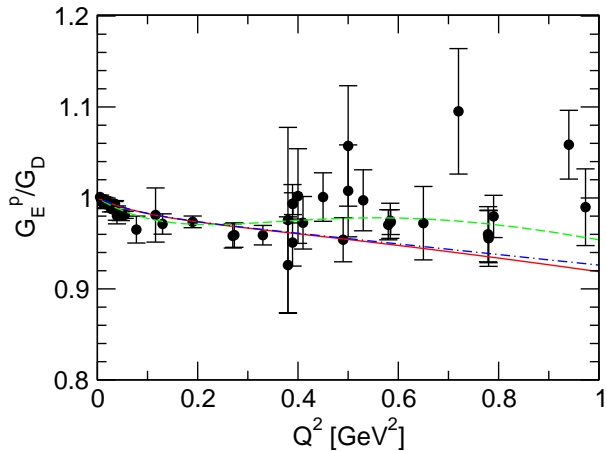


**Fig. 3.** The proton charge form factor  $G_E^p$  for momentum transfers  $Q^2 = 0 \dots 1 \text{ GeV}^2$ . The curves are as in Fig. 1.

The  $\omega NN$  and  $\phi NN$  coupling constants derived from the residues given above are  $g_1^{\omega NN} = 21.4$ ,  $g_2^{\omega NN} = 0.9$ ,  $g_1^{\phi NN} = -10.3$ , and  $g_2^{\phi NN} = -3.1$ . The absolute values of these coupling constants are comparable with the results of Refs. [1,2] but the small tensor couplings  $g_2^{\omega NN}$  and  $g_2^{\phi NN}$  have changed sign. This change of sign indicates that the error in the extracted vector meson coupling constants is of the order of the tensor couplings.

For the electric and magnetic radii of the nucleon, we find the values  $r_E^p = 0.848 \text{ fm}$ ,  $r_M^p = 0.857 \text{ fm}$ , and  $r_M^n = 0.879 \text{ fm}$ . As in the previous analysis [1,2], the proton charge radius is somewhat small compared to the recent precise determinations  $r_E^p = 0.880(15) \text{ fm}$  [5] and  $r_E^p = 0.895(18) \text{ fm}$  [6] from low-momentum-transfer data and  $r_E^p = 0.883(14) \text{ fm}$  [20] from Lamb shift measurements.

Note that the recent determinations of the proton charge radius by Rosenfelder [5] and Sick [6] are based on analyzing low-momentum cross section data directly and include corrections from two-photon exchange. Our analysis relies on form factor data extracted in the one-photon exchange approximation where the two-photon corrections enter in the systematical error. A comparison of our value to the analyses of low-momentum transfer cross sections directly allows one to estimate systematic errors in the extraction of the radii. Of course, one might contemplate a fit to cross section data only. However, for consistency the two-photon corrections have to be applied to the full data basis (as opposed to low  $Q^2$  data only) and this will certainly take a long time. This issue has to be addressed in the future but requires a large common effort by experimenters and theorists.

Our results for the magnetic radii of the proton and neutron are consistent with the recent values from continued fraction expansions: Kubon et al. [21] extracted  $r_M^n = 0.873(11) \text{ fm}$  from precise data for  $G_M^n$ , while Sick [6,22] obtained  $r_M^p = 0.855(35) \text{ fm}$  from a careful analysis of the world data on elastic electron-proton scattering. To simplify the comparison, we have collected our results and the other recent radius determinations in Table 1.

$r_E^p$ [fm]	$r_M^p$ [fm]	$r_M^n$ [fm]	Reference
0.848	0.857	0.879	this work
0.880(15)			[5]
0.895(18)	0.855(35)		[6,22]
0.883(14)			[20]
		0.873(11)	[21]

**Table 1.** Comparison of our results for the radii  $r_E^p$ ,  $r_M^p$ , and  $r_M^n$  with other recent determinations. The numbers in parentheses indicate the error in the last digits.

## 4 Outlook

We have shown that a dispersion-theoretical analysis based on a minimal number of poles can describe most of the current world data on the nucleon electromagnetic form factors for space-like momentum transfer. While the charge radius of the proton is still somewhat small, the magnetic radii of the proton and neutron are in good agreement with the recent determinations using continued fraction expansions [6,21,22].

The spectral functions used here can be improved. Ideally, one would like spectral functions consisting of various continuum contributions with vector mesons emerging naturally as resonances and avoid explicit pole terms altogether. In particular, the isoscalar region around masses of 1 GeV could be supplemented by explicit  $\pi\rho$  [23] and  $K\bar{K}$  [24] continuum contributions. The  $\phi$  meson would then appear as a finite width resonance in the  $K\bar{K}$  (and possibly  $\pi\rho$ ) continua, thereby eliminating the need to include it explicitly as a pole term. It would also be desirable to replace the poles with masses in the region from 1.5 to 2.0 GeV with an appropriate continuum contribution. However, the analytical continuation of experimental data that is required to obtain the continua becomes more and more difficult the higher one gets in mass, so that the latter goal is not realistic in the near future. Another improvement is to construct a better representation of the perturbative QCD behaviour for large  $Q^2$ . This would allow to include all existing time-like data in the fits, and thus lead to a more consistent description of these fundamental quantities.

Furthermore, the proton charge radius extracted from low-momentum-transfer data and Lamb shift measurements could be included as a further constraint in the analysis. This would allow to check the consistency between the high- $Q^2$  data and the low- $Q^2$  extractions of the radii. Whether this requires the introduction of additional vector meson poles is an open question. Last but not least, a full error analysis of the extracted radii and coupling constants should be carried out. As mentioned above, this is a nontrivial task because of the highly nonlinear nature of the problem. Work along these lines is under way [25].

## Acknowledgment

We acknowledge valuable discussions with D. Drechsel, J. Friedrich, I. Sick, and Th. Walcher. Furthermore, we thank J. Friedrich and Th. Walcher for providing us with their data basis and updated fit parameters.

## References

1. P. Mergell, U.-G. Meißner, and D. Drechsel, Nucl. Phys. A **596**, 367 (1996) [arXiv:hep-ph/9506375].
2. H.-W. Hammer, U.-G. Meißner, and D. Drechsel, Phys. Lett. B **385**, 343 (1996) [arXiv:hep-ph/9604294].
3. H.-Y. Gao, Int. J. Mod. Phys. E **12**, 1 (2003) [Int. J. Mod. Phys. E **12**, 567 (2003)] [arXiv:nucl-ex/0301002].
4. H. Schmieden, arXiv:nucl-ex/0302027.
5. R. Rosenfelder, Phys. Lett. B **479**, 381 (2000) [arXiv:nucl-th/9912031].
6. I. Sick, Phys. Lett. B **576**, 62 (2003) [arXiv:nucl-ex/0310008].
7. E. L. Lomon, Phys. Rev. C **64**, 035204 (2001) [arXiv:nucl-th/0104039].
8. S. Dubnicka, A. Z. Dubnickova, and P. Weisenpacher, J. Phys. G **29**, 405 (2003) [arXiv:hep-ph/0208051].
9. J. Friedrich and T. Walcher, Eur. Phys. J. A **17**, 607 (2003) [arXiv:hep-ph/0303054].
10. G. Höhler and E. Pietarinen, Nucl. Phys. B **95**, 210 (1975).
11. I. Sabba Stefanescu, J. Math. Phys. **21**, 175 (1980).
12. S. Kopecky, M. Krenn, P. Riehs, S. Steiner, J. A. Harvey, N. W. Hill, and M. Pernicka, Phys. Rev. C **56**, 2229 (1997).
13. M. K. Jones *et al.* [Jefferson Lab Hall A Collaboration], Phys. Rev. Lett. **84**, 1398 (2000) [arXiv:nucl-ex/9910005].
14. O. Gayou *et al.* [Jefferson Lab Hall A Collaboration], Phys. Rev. Lett. **88**, 092301 (2002) [arXiv:nucl-ex/0111010].
15. G. Höhler *et al.*, Nucl. Phys. B **114**, 505 (1976).
16. G. Höhler, "Pion-Nucleon Scattering", Landolt-Börnstein Vol. I/9b, ed. H. Schopper, Springer, Berlin, 1983.
17. U.-G. Meißner, Nucl. Phys. A **623**, 340c (1997) [arXiv:hep-ph/9611424].
18. H.-W. Hammer, in *Proc. of the  $e^+e^-$  Physics at Intermediate Energies Conference* ed. Diego Bettoni, eConf **C010430**, W08 (2001) [arXiv:hep-ph/0105337].
19. H.-W. Hammer, D. Drechsel, and U.-G. Meißner, Phys. Lett. B (in press) [arXiv:hep-ph/0310240].
20. K. Melnikov and T. van Ritbergen, Phys. Rev. Lett. **84**, 1673 (2000) [arXiv:hep-ph/9911277].
21. G. Kubon *et al.*, Phys. Lett. B **524**, 26 (2002) [arXiv:nucl-ex/0107016].
22. I. Sick, private communication.
23. U.-G. Meißner, V. Mull, J. Speth, and J. W. van Orden, Phys. Lett. B **408**, 381 (1997) [arXiv:hep-ph/9701296].
24. H.-W. Hammer and M. J. Ramsey-Musolf, Phys. Rev. C **60**, 045204 (1999) [Erratum-ibid. C **62**, 049902 (2000)] [arXiv:hep-ph/9903367]; Phys. Rev. C **60**, 045205 (1999) [Erratum-ibid. C **62**, 049903 (2000)] [arXiv:hep-ph/9812261].
25. M. Belushkin, H.-W. Hammer, and U.-G. Meißner, work in progress.